

Three commensurate magnetic structures in the solid solution $U(Ni_{0.25}Cu_{0.75})_2Si_2$, observed by neutron diffraction

Moshe Kuznietz

Nuclear Research Centre-Negev, P. O. Box 9001, 84190 Beer-Sheva, Israel
and Laboratoire Léon Brillouin (Commissariat à l'Énergie Atomique - Centre National de la Recherche Scientifique),
Centre d'Études de Saclay, 91191 Gif-sur-Yvette Cedex, France

Gilles André and Françoise Bourée

Laboratoire Léon Brillouin (Commissariat à l'Énergie Atomique - Centre National de la Recherche Scientifique),
Centre d'Études de Saclay, 91191 Gif-sur-Yvette Cedex, France

Haim Pinto, Hanania Etedgui, and Mordechai Melamud

Nuclear Research Centre-Negev, P.O. Box 9001, 84190 Beer-Sheva, Israel

(Received 1 March 1994)

A polycrystalline sample of the solid solution $U(Ni_{0.25}Cu_{0.75})_2Si_2$ was prepared and found to have the tetragonal $ThCr_2Si_2$ -type crystallographic structure. The observation of a ferrimagnetic transition at 112 ± 5 K by ac-susceptibility measurements, is confirmed by neutron diffraction, which also indicated three commensurate magnetic structures (below ≈ 110 K). Two structures are antiferromagnetic (AF), 40% each, and one is ferrimagnetic, 20% in volume. The structures are AF-I (+ - + -), ferrimagnetic (+ + -), and AF-IA (+ + - -), with wave vectors $\mathbf{k} = (0, 0, 1)$, $(0, 0, \frac{2}{3})$, and $(0, 0, \frac{1}{2})$, and $T_N = 120 \pm 3$, 115 ± 4 , and 110 ± 3 K, respectively. The uranium ordered magnetic moments ($2.2 \pm 0.1 \mu_B$ at 1.5 K) are along the tetragonal axis in all three structures. These phases fit well into the proposed magnetic phase diagram of the $U(Ni_{1-x}Cu_x)_2Si_2$ system, and are compared with corresponding solid solutions in the parallel $U(Ni_{1-x}Cu_x)_2Ge_2$ system.

I. INTRODUCTION

Our previous neutron-diffraction and ac-susceptibility studies of the magnetic structures in the ternary UNi_2Ge_2 and UCu_2Ge_2 compounds¹⁻⁴ and pseudoternary $U(Ni_{1-x}Cu_x)_2Ge_2$ solid solutions^{1,3-5} having the body-centered-tetragonal $ThCr_2Si_2$ -type crystallographic structure, resulted in the magnetic phase diagram of the $U(Ni,Cu)_2Ge_2$ system.⁴ Following earlier studies of the end-compounds UNi_2Si_2 and UCu_2Si_2 (Refs. 6 and 7), we have been working recently on the corresponding $U(Ni,Cu)_2Si_2$ system, beginning with the intermediate solid solution, $U(Ni_{0.50}Cu_{0.50})_2Si_2$, briefly termed $UNiCuSi_2$.^{8,9}

UNi_2Si_2 , as studied by neutron diffraction, earlier on a polycrystalline sample⁶ and more recently on a single crystal,⁷ is reported to order at $T_N = 124 \pm 1$ K into an incommensurate (IC) phase, with a wave vector $\mathbf{k} = (0, 0, k_z)$ that varies with temperature. It undergoes an incommensurate-commensurate phase transition at $T_{IC} = 103 \pm 1$ K to the antiferromagnetic AF-I (+ - + -) structure, with a wave vector $\mathbf{k} = (0, 0, 1)$, and undergoes another transition at $T_0 = 53 \pm 1$ K to a ferrimagnetic (+ + -) phase with a wave vector $\mathbf{k} = (0, 0, \frac{2}{3})$. The uranium magnetic moments are aligned along the tetragonal axis in all three magnetic phases. The IC phase has not been observed in the powder measurements.⁶ UCu_2Si_2 is reported by powder neutron diffraction⁶ to order ferromagnetically below $T_C = 103 \pm 3$ K, with moments, along the tetragonal axis, only on the uranium atoms.

We performed ac-susceptibility and neutron-diffraction measurements on two separately prepared $UNiCuSi_2$ samples.^{8,9} An antiferromagnetic (AF) transition at $T_N = 150 \pm 5$ K was observed in these measurements in both samples. The magnetic structure was determined by neutron diffraction to be AF-I, persisting down to 1.5 K. Additional transitions with a ferro/ferrimagnetic (F) character were observed by ac-susceptibility in $UNiCuSi_2$ (I) (at 110 ± 5 , 90 ± 5 , 70 ± 5 , and 45 ± 5 K) and in $UNiCuSi_2$ (II) (at 110 ± 5 , 60 ± 5 , and 45 ± 5 K). These F transitions were associated with short-range magnetic order involving only several consecutive ferromagnetic planes in the AF-I phase, and therefore detected by ac susceptibility but not by neutron diffraction.^{6,7}

We extend here our previous studies of the intermediate solid solution $UNiCuSi_2$ ($x = 0.50$)^{8,9} to another solid solution, $U(Ni_{0.25}Cu_{0.75})_2Si_2$ ($x = 0.75$), formed between the end-compounds UNi_2Si_2 and UCu_2Si_2 .

II. EXPERIMENTAL DETAILS

A polycrystalline sample of the solid solution $U(Ni_{0.25}Cu_{0.75})_2Si_2$ was prepared at the Nuclear Research Centre-Negev (NRCN) by arc-melting of stoichiometric amounts of the constituents in an argon atmosphere. The obtained button was annealed at 750°C in vacuum for 120 h, and was subsequently crushed into a fine powder and examined by x-ray diffraction at room temperature ($RT = 295$ K) to determine its quality, as well as its crystallographic structure and lattice parameters.

Ac-susceptibility measurements on a 380-mg sample were done at the NRCN in the temperature range 80–295 K. The ac magnetic field was rather weak (< 10 Oe). The ac-susceptibility values were calibrated with a 20-mg polycrystalline sample of Ho_2O_3 , for which χ_M at 293 K is 89×10^{-3} emu/mol (with $\theta = -14$ K and $\mu_{eff} = 10.5\mu_B$). These measurements provided a general classification of this material and its paramagnetic properties.

Neutron-diffraction measurements on a 20-g polycrystalline sample (in a cylindrical aluminium container) were done initially in the NRCN IRR-2 reactor, with the single-detector diffractometer KANDI-III ($\lambda = 2.40$ Å). A Displex (brand name of a closed-cycle helium cooler made by Air Products Inc.) was used for NRCN measurements down to 10 K. Due to the unresolved low-temperature (LT) neutron diffractogram, the neutron-diffraction measurements on $U(Ni_{0.25}Cu_{0.75})_2Si_2$ were also done on the G4.1 diffractometer (800 detectors, 0.1° apart) in the Orphée reactor of the Laboratoire Léon Brillouin (LLE) ($\lambda = 2.444$ Å). An Orange (ILL)-type cryostat was used for LLB measurements down to 1.5 K. These measurements were used to determine the RT and LT crystal structure, and LT magnetic structures.

III. RESULTS

At RT only $\{hkl\}$ reflections with $h+k+l = \text{even}$ were observed by x-ray and neutron diffraction from the $U(Ni_{0.25}Cu_{0.75})_2Si_2$ solid solution. These are consistent with the body-centered-tetragonal $ThCr_2Si_2$ -type crystallographic structure (space group $I4/mmm$), observed in all the UM_2X_2 compounds ($M = Co, Ni, Cu; X = Si, Ge$).^{6,10} The RT lattice parameters ($a = 3.980 \pm 0.010$ Å, $c = 9.77 \pm 0.02$ Å) and derived tetragonal cell volume ($V = 154.8$ Å³) of $U(Ni_{0.25}Cu_{0.75})_2Si_2$ fall between the respective values in the end-compounds UNi_2Si_2 and UCu_2Si_2 ,⁶ and are intermediate between those in $UNiCuSi_2$ (Refs. 8 and 9) and UCu_2Si_2 . For the RT NRCN neutron diffractogram (not shown) a least-squares fit of the observed integrated and calculated intensities yields random distribution of the Ni and Cu atoms in the $4d$ sites in $U(Ni_{0.25}Cu_{0.75})_2Si_2$, having $ThCr_2Si_2$ -type structure. The RT fitted position parameter of the Si atom is $z = 0.382 \pm 0.001$.

The temperature dependence of the molar ac susceptibility of the solid solution $U(Ni_{0.25}Cu_{0.75})_2Si_2$ in the temperature range 80–295 K, is shown in Fig. 1. A single transition to a ferrimagnetic state is observed at $T_N = 112 \pm 5$ K, with a value of $\chi_M = (82 \pm 4) \times 10^{-3}$ emu/mol at the transition, decreasing to $\chi_M = (4.1 \pm 0.2) \times 10^{-3}$ emu/mol at RT (ratio of ≈ 20). This ratio is ≈ 1000 in pure ferromagnets and only 2–3 in pure antiferromagnets. The paramagnetic Curie temperature θ of $U(Ni_{0.25}Cu_{0.75})_2Si_2$ is obtained from the intersection of the linear part (above 200 K) of the inverse susceptibility curve (Fig. 1) with the temperature axis. The effective paramagnetic moment μ_{eff} (in μ_B , Bohr magnetons) is obtained via the relation $(\chi_M)^{-1} = (2.83/\mu_{eff})^2(T - \theta)$, where χ_M is given in

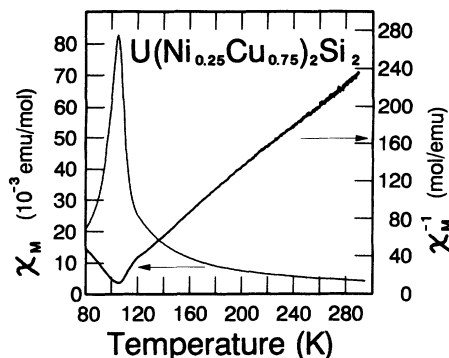


FIG. 1. Temperature dependence of the molar ac-susceptibility (thin line) and the inverse susceptibility (thick line) in a polycrystalline sample of the $U(Ni_{0.25}Cu_{0.75})_2Si_2$ solid solution, indicating an overall ferrimagnetic ordering below $T_N = 112 \pm 5$ K, and yielding paramagnetic values: $\theta = +80 \pm 10$ K and $\mu_{eff} = 2.7 \pm 0.2\mu_B$.

emu/mol and $(T - \theta)$ in K. The values obtained are $\theta = +80 \pm 10$ K and $\mu_{eff} = 2.7 \pm 0.2\mu_B$, and these are compatible with the respective values in UNi_2Si_2 ,^{6,7} $UNiCuSi_2$,^{8,9} and UCu_2Si_2 .^{6,11}

The LT neutron diffractogram (at ≈ 10 K) of $U(Ni_{0.25}Cu_{0.75})_2Si_2$, obtained at the NRCN (not shown), contained several additional reflections for which

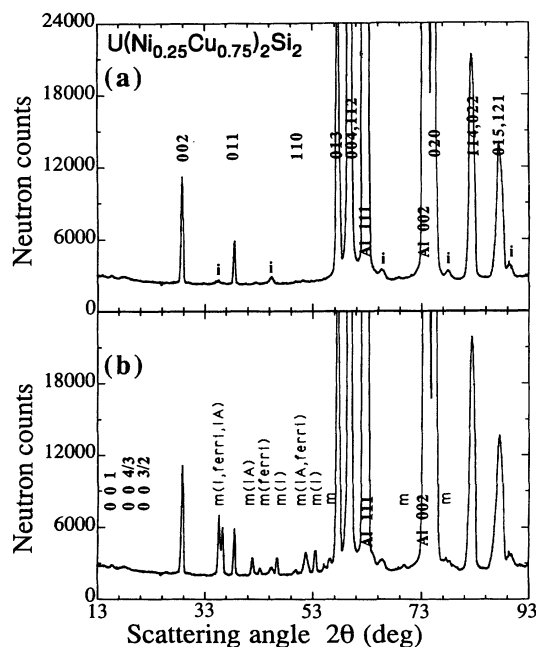


FIG. 2. Neutron ($\lambda = 2.444$ Å at LLB) diffraction patterns ($2\theta = 13\text{--}93^\circ$) of a polycrystalline sample of $U(Ni_{0.25}Cu_{0.75})_2Si_2$: (a) at 130 K—indicating a $ThCr_2Si_2$ -type major phase, and small impurity-phase reflections (denoted by “?”); (b) at 1.5 K—showing additional magnetic reflections which pertain to the AF-I, ferrimagnetic, and AF-IA magnetic structures, and the absence of $\{00l\}$ reflections except for those with even l ; (aluminium reflections from the sample container and the cryostat are marked).

$h+k+l$ is not even. Some of the additional reflections could be indexed as $\{hkl\}$ with $h+k+l=\text{odd}$ (such as $\{010\}$, $\{012\}$, and $\{111\}$), or alternatively as $\{hk(l\pm 1)\}$ satellites of the $\{hkl\}$ nuclear reflections, indicating AF ordering of at least the uranium sublattice, with a wave vector $\mathbf{k}=(0,0,1)$ and alternate stacking (+-) of ferromagnetic uranium planes along the tetragonal axis (AF-I). Other additional reflections could perhaps be indexed $\{hk[l\pm(\frac{1}{2})]\}$ [such as $\{01(\frac{1}{2})\}$, $\{01(\frac{3}{2})\}$, $\{01(\frac{5}{2})\}$, $\{11(\frac{1}{2})\}$, $\{11(\frac{3}{2})\}$, $\{11(\frac{5}{2})\}$], as satellites of the $\{hkl\}$ nuclear reflections, indicating AF ordering of at least the uranium sublattice, with a wave vector $\mathbf{k}=(0,0,1/2)$ and (+ + - -) stacking of ferromagnetic planes along the tetragonal axis (AF-IA). Yet additional reflections could not be accounted for due to the poor statistical quality in this situation of coexisting magnetic reflection sets.

In order to resolve the magnetic structure of $\text{U}(\text{Ni}_{0.25}\text{Cu}_{0.75})_2\text{Si}_2$, further neutron-diffraction measurements were done at the LLB, using the 800-detectors of the G4.1 diffractometer with its superior resolution. The LLB neutron diffractograms in the paramagnetic state (at 130 K) and in the ordered state (at 1.5 K) are shown for the entire measurement range ($2\theta=13-93^\circ$) in Figs. 2(a) and 2(b), and for the magnetically interesting range ($2\theta=33-57^\circ$) in Figs. 3(a) and 3(b), respectively. Fitting of the LLB neutron diffractograms in the temperature range of 1.5–130 K to the respective calculated spectra was achieved by the modified Rietveld refinement analysis.¹²

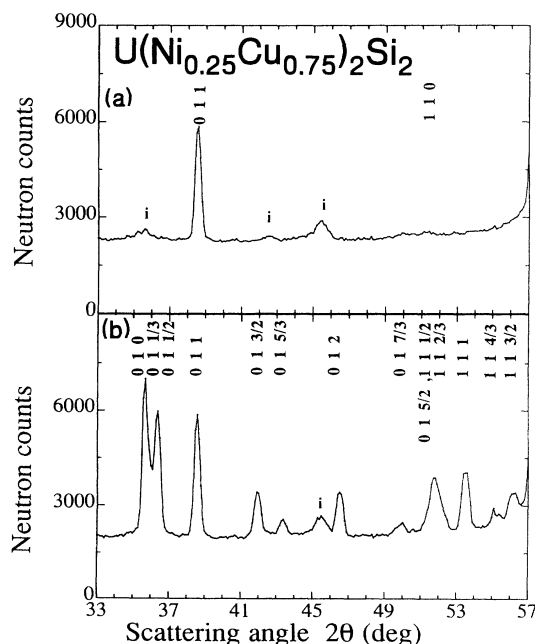


FIG. 3. Enlarged range ($2\theta=33-57^\circ$) of the neutron ($\lambda=2.444 \text{ \AA}$ at LLB) diffraction patterns of a polycrystalline sample of $\text{U}(\text{Ni}_{0.25}\text{Cu}_{0.75})_2\text{Si}_2$: (a) at 130 K—depicting the $\{011\}$ and $\{110\}$ reflections of the ThCr_2Si_2 -type major phase and three small impurity-phase reflections (denoted by “i”); (b) at 1.5 K—showing additional magnetic reflections which can be classified into three sets, as listed in Table I.

In addition to the nuclear $\{hkl\}$ reflections with $h+k+l=\text{even}$, seen in Figs. 2(a) and 3(a), three sets of magnetic reflections are classified, which are indexed as $\{hk(l\pm k_z)\}$ satellites of the $\{hkl\}$ reflections, with $k_z=1, \frac{2}{3}$, and $\frac{1}{2}$ [Figs. 2(b) and 3(b)]. The respective wave vectors $\mathbf{k}=(0,0,1)$, $(0,0,\frac{2}{3})$, and $(0,0,\frac{1}{2})$ correspond to the AF-I (+ - + -) and ferrimagnetic (+ + -) structures, already existing in UNi_2Si_2 ,^{6,7} and the AF-IA (+ + - -) structure. The latter is new in the system $\text{U}(\text{Ni}_{1-x}\text{Cu}_x)_2\text{Si}_2$, but was found previously in $\text{U}(\text{Ni}_{0.05}\text{Cu}_{0.95})_2\text{Ge}_2$ (Ref. 4) and in a certain sample of UCu_2Ge_2 .⁶ The allowed reflections of the three coexisting magnetic structures are listed in Table I. The absence of $\{00(l\pm k_z)\}$ reflections, being satellites of nuclear $\{00l\}$ reflections (even l), notably the $\{001\}$, $\{00(\frac{4}{3})\}$, and $\{00(\frac{5}{2})\}$ reflections [Fig. 2(b), listed fully in Table I], indicates the alignment of all (uranium) ordered magnetic moments along the tetragonal c axis.

The first magnetic reflection in $\text{U}(\text{Ni}_{0.25}\text{Cu}_{0.75})_2\text{Si}_2$ [Fig. 2(b)] is a combination of the first reflections of the three sets, being the three satellites of the nuclear reflection $\{011\}$, namely $\{010\}$, $\{01(\frac{1}{3})\}$, and $\{01(\frac{1}{2})\}$, respectively, which are too close to be completely resolved even in the LLB measurements (see 2θ values in Table I). The first resolved satellites of the three reflection sets are $\{012\}$, $\{01(\frac{5}{3})\}$, and $\{01(\frac{3}{2})\}$, respectively, followed by other reflections of these sets, as detailed in Table I. The detection of the resolved $\{01(\frac{5}{3})\}$ and $\{01(\frac{7}{3})\}$ reflections in the LLB diffractogram [Fig. 3(b)], which could not be identified in the NRCN LT diffractogram, suggested the existence of the ferrimagnetic (+ + -) phase with the two AF phases. Such a coexistence explains the overall ferrimagnetic behavior of the material, as suggested by its ac susceptibility (Fig. 1).

The treatment of the LLB LT (=1.5 K) neutron diffractogram [Fig. 2(b)] with the modified Rietveld refinement analysis¹² takes into account four phases: the (paramagnetic) nuclear phase and three, identified-above, commensurate magnetic phases: AF-I (+ - + -), ferrimagnetic (+ + -), and AF-IA (+ + - -) (with 10, 5, 17, and 11 Bragg reflections, respectively, listed fully in Table I). As at least $\frac{1}{5}$ of the entire volume of the present sample is ferrimagnetic (+ + -), it leads to magnetic contributions to all nuclear reflections except $\{002\}$, which are, however, quite small.

The LLB LT lattice parameters obtained by the Rietveld procedure are $a=3.967\pm 0.001 \text{ \AA}$; $c=9.777\pm 0.002 \text{ \AA}$; $z=0.386\pm 0.001$. These are in agreement with above-mentioned NRCN RT lattice parameters.

The magnetic form factor of uranium in the three magnetic phases is approximated by the exponentially decreasing function, $\exp[-4.8(\sin\theta/\lambda)^2]$, used previously for UCo_2Ge_2 (Ref. 10) and subsequently for all $\text{U}(M,M')_2\text{X}_2$ materials.¹⁻⁵ Using the modified Rietveld profile analysis (at 1.5 K), the ordered-magnetic-moment contributions of the three magnetic phases to the entire sample are $m_1=1.35\pm 0.05\mu_B$ from the AF-I phase, $m_2=1.04\pm 0.07\mu_B$ from the ferrimagnetic phase, and $m_3=1.41\pm 0.05\mu_B$ from the AF-IA phase.

TABLE I. Classification of allowed $\{hkl\}$ neutron ($\lambda=2.444$ Å) Bragg reflections (denoted by an asterisk) in $ThCr_2Si_2$ -type polycrystalline sample of $U(Ni_{0.25}Cu_{0.75})_2Si_2$ according to the nuclear phase and the three coexisting magnetic phases: AF-I, ferrimagnetic, and AF-IA. The region $2\theta=61.6-78.0^\circ$ is excluded due to the presence of aluminium. The 0 (zero) magnetic reflections are due to ordered magnetic moments along the tetragonal axis.

h	k	l	2θ (deg)	Classified reflections by phases			
				Nuclear	AF-I	Ferri	AF-IA
0	0	$\frac{1}{2}$	7.11				0
0	0	$\frac{2}{3}$	9.49			0	
0	0	1	14.25		0		
0	0	$\frac{4}{3}$	19.04			0	
0	0	$\frac{5}{2}$	21.45				0
0	0	2	28.73	*			
0	1	0	35.61		*		
0	1	$\frac{1}{3}$	35.94			*	
0	0	$\frac{5}{2}$	36.14				0
0	1	$\frac{1}{2}$	36.36				*
0	1	1	38.53	*		*	
0	0	$\frac{8}{3}$	38.64			0	
0	1	$\frac{3}{2}$	41.95				*
0	1	$\frac{5}{3}$	43.32			*	
0	0	3	43.70		0		
0	1	2	46.38		*		
0	0	$\frac{10}{3}$	48.86			0	
0	1	$\frac{7}{3}$	49.80			*	
1	1	0	51.24	*		*	
0	0	$\frac{7}{2}$	51.47				0
0	1	$\frac{5}{2}$	51.64				*
1	1	$\frac{1}{2}$	51.80				*
1	1	$\frac{2}{3}$	52.24			*	
1	1	1	53.47		*		
1	1	$\frac{4}{3}$	55.16			*	
1	1	$\frac{3}{2}$	56.16				*
0	1	3	57.59	*		*	
0	0	4	59.50	*			
1	1	2	59.81	*		*	
0	2	$\frac{4}{3}$	78.61			*	
0	1	$\frac{9}{2}$	79.07				*
0	2	$\frac{3}{2}$	79.46				*
1	1	4	82.33	*		*	
0	2	2	82.59	*		*	
0	0	$\frac{16}{3}$	82.85			0	
0	0	$\frac{11}{2}$	86.05				0
1	2	0	86.26		*		
1	2	$\frac{1}{3}$	86.46			*	
0	2	$\frac{2}{2}$	86.57				*
1	2	$\frac{1}{2}$	86.71				*
0	1	5	87.51	*		*	
1	2	1	88.03	*		*	
0	2	$\frac{8}{3}$	88.10			*	
1	1	$\frac{9}{2}$	89.84				*
1	2	$\frac{3}{2}$	90.23				*
1	2	$\frac{5}{3}$	91.17			*	
0	2	3	91.43		*		
Number of reflections				10	5	17	11

Assuming that the ordered magnetic moment M on the uranium atoms is the same in all three magnetic phases, and that the contributions of these phases are proportional to their relative partial volumes v_1 , v_2 , and v_3 , respectively, (with $v_1+v_2+v_3=1$), we deduce the common moment and the relative partial volumes of the magnetic phases from the relations: $v_1M^2=m_1^2$; $v_2M^2=m_2^2$; $v_3M^2=m_3^2$; and from their sum: $M^2=m_1^2+m_2^2+m_3^2$. The deduced uranium ordered magnetic moment is $M=2.2\pm 0.1\mu_B$. The deduced relative partial volumes of the three coexisting magnetic phases are $v_1=0.37\pm 0.03$, $v_2=0.22\pm 0.03$, and $v_3=0.41\pm 0.04$. The uranium ordered magnetic moment (at 1.5 K) is comparable to the published values^{6,7,10,11} of the respective moments (at 4.2 to 10 K) in the UM_2X_2 compounds. The volume proportions in $U(Ni_{0.25}Cu_{0.75})_2Si_2$ of the coexisting magnetic phases at 1.5 K ($\approx 40:20:40$) are exhibited by the first combined magnetic reflection (Fig. 4), with its deconvoluted form at 1.5 K [Fig. 4(b)].

The temperature variation of the first combined magnetic reflection in $U(Ni_{0.25}Cu_{0.75})_2Si_2$ is shown in Fig. 4(a) for several of the LLB neutron diffractograms in the temperature range 1.5–130 K. Different variations of the $\{010\}$, $\{01(\frac{1}{3})\}$, and $\{01(\frac{1}{2})\}$ components for the AF-I

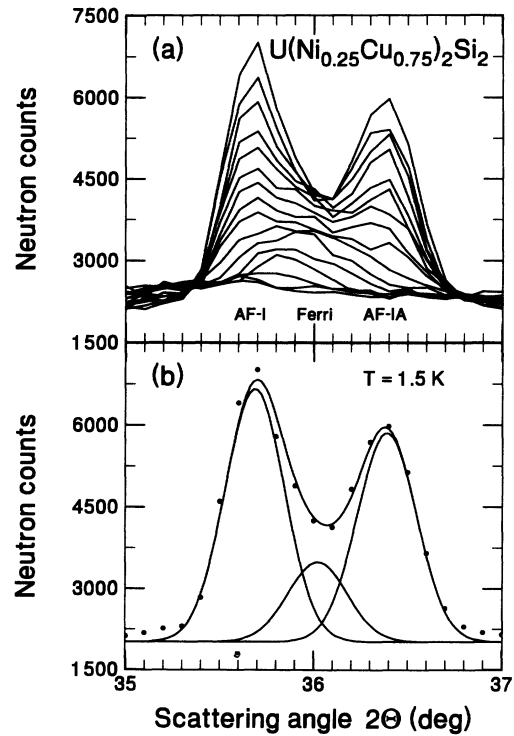


FIG. 4. The first combined magnetic reflection of the neutron ($\lambda=2.444$ Å) diffractograms ($2\theta=35-37^\circ$) of $U(Ni_{0.25}Cu_{0.75})_2Si_2$: (a) at 1.5 K (upper curve) and in the temperature range 71–130 K (curves decreasing, background rising with temperature), indicating different variations for the AF-I (+ - + -), ferrimagnetic (+ + -), and AF-IA (+ + - -), phases, the latter disappearing at $T_N=110\pm 3$ K and the others—at higher temperatures, with a possible relative increase in the ferrimagnetic phase. (b) at 1.5 K, with the deconvoluted reflections.

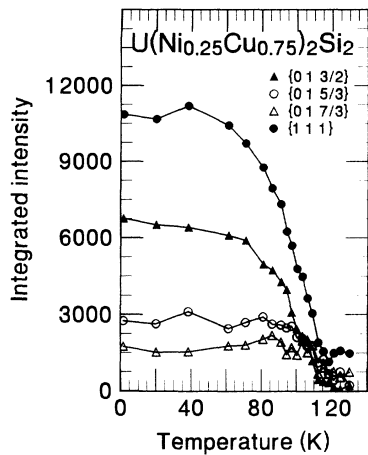


FIG. 5. Temperature dependence of the integrated intensity (above the background) of the magnetic reflections $\{01(\frac{3}{2})\}$ (AF-IA phase), $\{01(\frac{5}{3})\}$ and $\{01(\frac{7}{3})\}$ (ferrimagnetic phase), and $\{111\}$ (AF-I phase) in polycrystalline $U(Ni_{0.25}Cu_{0.75})_2Si_2$.

($+-+-$), ferrimagnetic ($++-$), and AF-IA ($++--$) phases, respectively, are noticed, the AF-IA phase disappearing first, at $T_N=110\pm 3$ K, and the others, at slightly higher temperatures, with a possible relative increase in the partial volume of the ferrimagnetic phase.

Temperature variations of the integrated neutron-diffraction intensities (above the background) of the separate magnetic reflections $\{01(\frac{3}{2})\}$ (of the AF-IA phase), $\{01(\frac{5}{3})\}$, and $\{01(\frac{7}{3})\}$ (of the ferrimagnetic phase), and $\{111\}$ (of the AF-I phase) in $U(Ni_{0.25}Cu_{0.75})_2Si_2$ are plotted in Fig. 5. The curve for the $\{01(\frac{3}{2})\}$ reflection in Fig. 5 yields $T_N=110\pm 3$ K for the AF-IA ($++--$) phase, in agreement with the transition temperature of the $\{01(\frac{1}{2})\}$ component of the first (combined) reflection [Fig. 4(a)]. The curve for the $\{111\}$ reflection in Fig. 5 yields the highest transition temperature, $T_N=120\pm 3$ K, for the AF-I ($+-+-$) phase. By close examination of the curves for the small reflections, $\{01(\frac{5}{3})\}$ and $\{01(\frac{7}{3})\}$, in Fig. 5 we deduce the transition temperature $T_N=115\pm 4$ K for the ferrimagnetic ($++-$) phase. It is this last transition that is reflected in the strong ac-susceptibility peak at the intermediate temperature, 112 ± 5 K (Fig. 1).

IV. DISCUSSION

The coexistence of two magnetic phases, commensurate or incommensurate, at a first-order magnetic transition between them is a common feature in compounds or solid solutions with such magnetic transitions. In such cases the coexistence of magnetic structures takes place in a limited temperature range, which is narrow in single-crystal samples and wider—in polycrystalline samples of these materials. This is the situation in UNi_2Si_2 , where the above-mentioned (Sec. I) studies of polycrystalline⁶ and single-crystal⁷ samples showed the coexistence

of the AF-I ($+-+-$) and ferrimagnetic ($++-$) structures around the first-order transition at $T_0=53\pm 1$ K, while the study of the single-crystal sample⁷ showed the coexistence of the incommensurate and AF-I (commensurate) structures around the first-order transition at $T_{IC}=103\pm 1$ K. Among the binary NaCl-type uranium monopnictides and monochalcogenides, UAs was studied by powder¹³ and single-crystal¹⁴ neutron diffraction and a coexistence of two commensurate magnetic phases was found at the first-order magnetic transition between the AF type-I ($+-+-$) and AF type-IA ($++--$) structures, characterized by wave vectors $\mathbf{k}=(0,0,1)$ and $(0,0,\frac{1}{2})$, above and below the transition at $T_0=63\pm 1$ K, respectively.

The coexistence of several commensurate magnetic phases in a wide range of temperatures, up to the entire ordered state, is not as common, but can take place in solid-solution systems for certain nominal compositions, in complex regions of the respective magnetic phase diagrams. This is an inherent property of solid solutions, either in polycrystalline or single-crystal materials, due to the existence of finite range of compositions around the nominal composition, throughout the samples.

Examples for this situation are the widely studied NaCl-type systems of $UAs_{1-x}Se_x$ (Ref. 15) and $UP_{1-x}S_x$ (Ref. 16) solid solutions. A coexistence of two commensurate magnetic phases in $UAs_{0.96}Se_{0.05}$ single crystal was observed¹⁷ in the temperature range 93–103 K, with the AF type-I ($+-+-$) and AF type-IA ($++--$) structures, characterized by wave vectors $\mathbf{k}=(0,0,1)$ and $(0,0,\frac{1}{2})$, respectively. A coexistence of up to four magnetic phases in $UP_{0.75}S_{0.25}$ single crystal was observed¹⁶ below $T=25$ K, with the AF type-IA ($2+,2-$), (probably) ferrimagnetic ($5+,4-$), AF ($5+,5-$), and ferromagnetic structures, characterized by wave vectors $\mathbf{k}=(0,0,\frac{1}{2})$, $(0,0,\frac{2}{3})$, $(0,0,\frac{1}{3})$, and $(0,0,0)$, respectively.

In the present study we have observed three coexisting commensurate magnetic phases in our polycrystalline sample of $U(Ni_{0.25}Cu_{0.75})_2Si_2$ (nominal copper content of 0.7) with the AF-I ($+-+-$), ferrimagnetic ($++-$), and AF-IA ($++--$) structures, characterized by the wave vectors $\mathbf{k}=(0,0,1)$, $(0,0,\frac{2}{3})$, and $(0,0,\frac{1}{2})$, respectively. This observation points out to a complex region of the magnetic phase diagram of the $U(Ni_{1-x}Cu_x)_2Si_2$ system in the vicinity of $x=0.75$, with the AF-I structure for $x<0.75$ (extending the same structure for $x=0.50$), the AF-IA structure for $x>0.75$, and the ferrimagnetic ($++-$) structure in a narrow x range in between. These three commensurate magnetic structures are observed also in the parallel $U(Ni_{1-x}Cu_x)_2Ge_2$ system, in which they appear in three different solid solutions around the successive nominal compositions $x=0.75$ (AF-I), $x=0.90$ (ferrimagnetic), and $x=0.95$ (AF-IA). As seen from the relevant part of the magnetic phase diagram of the $U(Ni_{1-x}Cu_x)_2Ge_2$ system [Fig. 6(a)], the transition from the paramagnetic state into the different ordered states proceeds via a ferromagnetic state. Such a ferromagnetic structure is not observed in the present $U(Ni_{1-x}Cu_x)_2Si_2$ system, as seen from the relevant part of its magnetic phase diagram [Fig. 6(b)], where the three

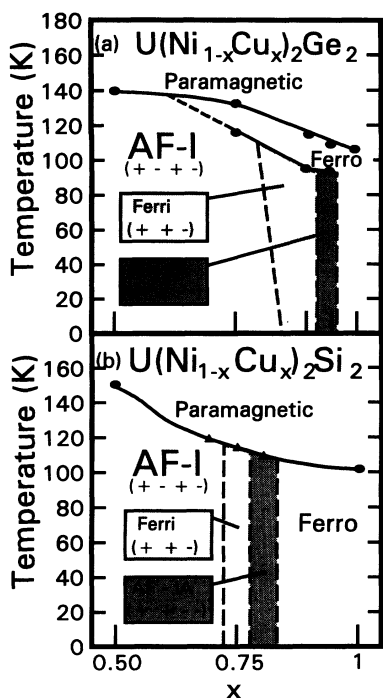


FIG. 6. The copper-rich side ($0.5 \leq x \leq 1$) of the magnetic phase diagram (temperature versus composition) of the solid-solution systems: (a) $U(Ni_{1-x}Cu_x)_2Ge_2$; (b) $U(Ni_{1-x}Cu_x)_2Si_2$. The boundaries between phases are approximate, and so are the positions of the three triangles at 110–120 K for $x=0.75$ in case (b) [representing the coexisting phases in $U(Ni_{1-x}Cu_x)_2Si_2$, with nominal $x=0.75$].

magnetic structures appear in one sample with a nominal $x=0.75$.

From the ac-susceptibility measurements it is clear that the sample of $U(Ni_{0.25}Cu_{0.75})_2Si_2$ orders ferrimagnetically at $T_N = 112 \pm 5$ K. As only $\frac{1}{5}$ of the sample is ferrimagnetic at 1.5 K, and this phase exhibits in the bulk

only $\frac{1}{3}$ of the uranium ordered magnetic moment, the χ_M at the transition should be approximately $\frac{1}{15}$ of the χ_M value at the ordering temperature of a fully ferromagnetic UM_2X_2 material, assuming that the contributions of the antiferromagnetic phases are negligible. In UCu_2Ge_2 this value is 4300×10^{-3} emu/mol,⁴ yielding a correct order-of-magnitude estimate for χ_M at the transition in the present $U(Ni_{0.25}Cu_{0.75})_2Si_2$ sample, bearing in mind that at T_N the proportion of the three phases may be different from that at 1.5 K.

The three commensurate magnetic phases observed in $U(Ni_{0.25}Cu_{0.75})_2Si_2$ involve uranium magnetic moments, aligned along the tetragonal axis and ordered in ferromagnetic basal planes. This form of exchange is related to the stronger $5f$ - $6d$ hybridization and shortest U-U distances in the basal planes (equal to the lattice parameter a). The transition between any two of these phases takes place by reversing the direction of the magnetic moments of entire uranium planes, on half of such planes in the crystal.

The actual stacking of the ferromagnetic uranium planes in the various magnetic structures is closely related to the number of conduction electrons, which varies with x , via Ruderman-Kittel-Kasuya-Yosida-type interactions as discussed for the parallel $U(Ni_{1-x}Cu_x)_2Ge_2$ system.⁴ In the $U(Ni_{1-x}Cu_x)_2Si_2$ system around $x=0.75$ small variations of x cause appreciable changes in the magnetic structure, thereby confirming the complex magnetic situation in this composition region.

The placement of coexisting magnetic structures of $U(Ni_{0.25}Cu_{0.75})_2Si_2$ in the $U(Ni_{1-x}Cu_x)_2Si_2$ system, in the order presented in Fig. 6(b) of decreasing k_z component of the wave vector $\mathbf{k}=(0,0,k_z)$ will be further investigated with solid solutions of nominal $x=0.70$ and 0.80 , on either sides of the present solid solution. According to the above considerations the sample with $x=0.70$ is expected to order mostly in the magnetic AF-I structure, while the sample with $x=0.80$ is expected to order mostly in the magnetic AF-IA structure.

¹M. Kuznietz, H. Pinto, and M. Melamud, *J. Appl. Phys.* **67**, 4808 (1990).

²M. Kuznietz, H. Pinto, and M. Melamud, *J. Magn. Magn. Mater.* **83**, 321 (1990).

³M. Kuznietz, H. Pinto, H. Ettetdgui, and M. Melamud, *J. Magn. Magn. Mater.* **104-107**, 13 (1992).

⁴M. Kuznietz, H. Pinto, H. Ettetdgui, and M. Melamud, *Phys. Rev. B* **48**, 3183 (1993).

⁵M. Kuznietz, H. Pinto, H. Ettetdgui, and M. Melamud, *Phys. Rev. B* **45**, 7282 (1992).

⁶L. Chelmsicki, J. Leciejewicz, and A. Zygmunt, *J. Phys. Chem. Solids* **46**, 529 (1985).

⁷H. Lin, L. Rebelsky, M. F. Collins, J. D. Garrett, and W. J. L. Buyers, *Phys. Rev. B* **43**, 13 232 (1991).

⁸M. Kuznietz, G. André, F. Bourée, H. Pinto, H. Ettetdgui, and M. Melamud, *J. Appl. Phys.* **73**, 6075 (1993).

⁹M. Kuznietz, G. André, F. Bourée, H. Pinto, H. Ettetdgui, and M. Melamud, *Solid State Commun.* **87**, 689 (1993).

¹⁰M. Kuznietz, H. Pinto, H. Ettetdgui, and M. Melamud, *Phys. Rev. B* **40**, 7328 (1989).

¹¹K. Hiebl and P. Rogl, *J. Nucl. Mater.* **144**, 193 (1987).

¹²J. Rodriguez-Carvajal, *Physica B* **192**, 55 (1993).

¹³J. Leciejewicz, A. Murasik, and R. Troc, *Phys. Status Solidi* **30**, 157 (1968).

¹⁴J. Rossat-Mignod, P. Burlet, H. Bartholin, R. Tchapoutian, O. Vogt, C. Vettier, and R. Lagnier, *Physica* **102B**, 177 (1980).

¹⁵M. Kuznietz, P. Burlet, J. Rossat-Mignod, and O. Vogt, *J. Magn. Magn. Mater.* **69**, 12 (1987).

¹⁶M. Kuznietz, P. Burlet, J. Rossat-Mignod, and O. Vogt, *J. Magn. Magn. Mater.* **63&64**, 165 (1987).

¹⁷M. Kuznietz, P. Burlet, J. Rossat-Mignod, and O. Vogt, *J. Magn. Magn. Mater.* **61**, 246 (1986).

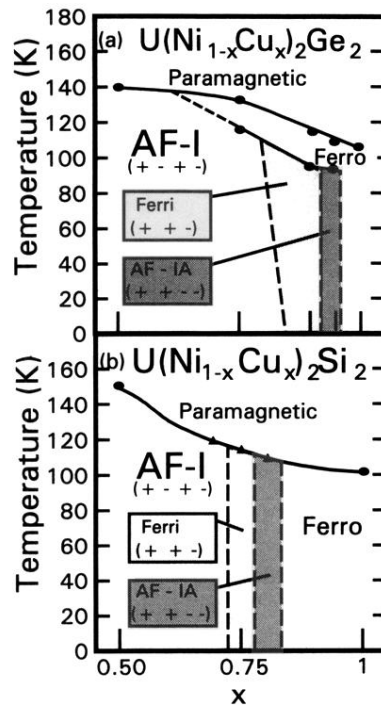


FIG. 6. The copper-rich side ($0.5 \leq x \leq 1$) of the magnetic phase diagram (temperature *versus* composition) of the solid-solution systems: (a) $U(Ni_{1-x}Cu_x)_2Ge_2$; (b) $U(Ni_{1-x}Cu_x)_2Si_2$. The boundaries between phases are approximate, and so are the positions of the three triangles at 110–120 K for $x=0.75$ in case (b) [representing the coexisting phases in $U(Ni_{1-x}Cu_x)_2Si_2$, with nominal $x=0.75$].